



## Bioactive biodegradable polycaprolactone implant for management of osteochondral defects: an experimental study

A.V. Popkov, E.S. Gorbach<sup>✉</sup>, E.N. Gorbach, N.A. Kononovich, E.A. Kireeva, D.A. Popkov

Ilizarov National Medical Research Centre for Traumatology and Orthopedics, Kurgan, Russian Federation

**Corresponding author:** Evgenij S. Gorbach, gorbach.evg@mail.ru

### Abstract

**Introduction** Repair of the affected articular surface still remains an unsolved problem. **The purpose** of this study was to assess the efficacy of a biodegradable polycaprolactone implant coated with hydroxyapatite on the healing of an osteochondral defect of the femoral condyle in rats. **Materials and methods** An osteochondral defect of the medial femoral condyle was modeled in 76 Wistar rats divided into 2 groups. In the experimental group, the defect was replaced with a biodegradable polycaprolactone membrane coated with hydroxyapatite. In the control group, the defect remained untreated. The results were assessed within a year. **Results** In the experimental group, the animals had a significantly better range of motion at all stages of the experiment than the control animals. The implant ensured the integrity and congruence of the articular surface. On day 180, a newly formed area of the articular surface of the organotypic structure was observed in the defect. Biomechanical properties of the repaired zone restored after 60 days while in the control one they remained lower by 27-29 %. **Discussion** Filling the defect with an elastic implant made of polycaprolactone with hydroxyapatite provided early functional load on the joint. The structure of the implant, simulating the extracellular matrix, promoted the growth, proliferation and directed differentiation of cells in the area of the osteochondral defect. The moderate rate of biodegradability of the material provided gradual replacement of the implant with organ-specific tissues. **Conclusion** A biodegradable polycaprolactone implant impregnated with hydroxyapatite particles might be effective for experimental osteochondral defect repair. **Keywords:** articular cartilage, osteochondral defect, biodegradable implants, polycaprolactone, hydroxyapatite

**For citation:** Popkov AV, Gorbach ES, Gorbach EN, Kononovich NA, Kireeva EA, Popkov DA. Bioactive biodegradable polycaprolactone implant for management of osteochondral defects: an experimental study. *Genij Ortopedii*. 2023;29(6):615-628. doi: 10.18019/1028-4427-2023-29-6-615-628

## INTRODUCTION

Lesions of joint articular cartilage are a common pathology of the musculoskeletal system. An analysis of more than 30,000 arthroscopic interventions associated with injuries and diseases of large joints showed pathological changes in the cartilage of varying severity in 63 % of cases [1, 2]. Focal disorders of the articular cartilage and subchondral bone of the femoral condyles mostly result from injuries or diseases of the knee joint. Their delayed or inadequate treatment could lead to the development of degenerative joint disorders [3].

Osteochondral defects of large joints frequently require surgical treatment [4]. Despite the fact that a wide range of surgical techniques for the treatment of articular cartilage has been introduced into clinical practice, the search for methods of articular surface repair remains a very urgent and unsolved problem at the present stage of medicine and biotechnology [5].

The low ability of the cartilage to regenerate has been proven by many researchers and is associated with the lack of blood supply and innervating components in it. Therefore, a lot of research has been and is being carried out to develop new methods, which, as a rule, are aimed at stimulating the repair and articular cartilage recovery [6, 7].

To date, one of the most efficient and cost-effective methods is the microfracturing method in its various modifications. However, the regenerate thus formed

in the subchondral defect area frequently undergoes lysis in patients older than 35 years [8, 9].

Mosaic chondroplasty contributes to the successful long-term repair of the damaged site with bone and cartilage autografts taken from unloaded areas of the articular surface [10, 11], but it can cause pain and degenerative changes in those areas, or they need to be filled with other implant materials, which requires additional costs and increases the time of the surgery.

In recent years, cell technologies have been successfully applied such as autologous chondrocyte implantation (ACI) into the area of the cartilage defect or a combination of autologous chondrocytes and collagen matrices (MACI) [12]. The shortcomings of these methods is complexity and high costs.

An alternative method for treating osteoarthritis is matrix-induced technologies (autologous membrane-induced chondrogenesis collagen, AMIC), when native bone marrow cells and poorly differentiated perivascular cells penetrate into the defect area as a result of preliminary microfracturing and further populate the implanted biocompatible biodegradable matrices. Current publications are mainly devoted to the results of replacement of cartilage defects with collagen matrices. However, natural collagen matrices are quite expensive and not always effective in the long term [13-15].

There are recent publications on the successful use of synthetic polymeric biodegradable implant materials, which are much cheaper and do not cause immune reactions [16-21]. However, complex experimental studies with a long-term follow-up period are required to objectively substantiate the use of such materials and technologies before introducing them in clinical practice.

## MATERIALS AND METHODS

The study was conducted on 76 Wistar rats, whose age was 7 months at the beginning of the experiment. Osteochondral defects of the articular surface of the medial femoral condyle were modeled in all the animals divided into 2 groups, 38 rats each. The knee joint was approached and an osteochondral defect of the medial condyle of the femur, 1.5-2 mm wide and 2 mm deep, was modeled using a 2-mm cutter. In the experimental group, the defect was filled with a biodegradable polycaprolactone (PCL) membrane with hydroxyapatite (a biodegradable elastic PCL matrix produced by electrospinning and containing hydroxyapatite). In the control group, the defects were left untreated. Surgical interventions were performed in a sterile operating room under general anesthesia (Rometar 2 % – 1-2 mg/kg, Bioveta, Czech Republic; Zoletil 100 – 10-15 mg/kg, Virbac Sante Animale, France). Five rats were intact to calculate reference normal values.

### *Clinical methods*

Clinical observation of all animals was carried out throughout the experiment. Their general condition and physical activity were assessed. Body weight was measured using electronic scales; general and local temperature in the area of surgical intervention and in the similar area of the contralateral limb was measured with a remote medical infrared thermometer (BWell Swis AG, Switzerland). The external condition of the lower leg soft tissues in the surgical area and the functional state of the limb were assessed. The circumference of the lower leg in its upper third was measured with a centimeter tape. The angles of passive knee extension and flexion were measured with a standard goniometer.

Defect healing was studied using microanatomical and histological methods. The animals were euthanized by an overdose of barbiturates after premedication with conventional pharmacological preparations on experiment days 14, 60, 180 and 360.

### *Anatomical methods*

After euthanasia, the femur of the involved limb was isolated and the femur soft tissues were dissected. In the area of the metaphysis, its distal articular end was sawn off with a cutter. The features of the articular surface defect and the whole articular surface were examined, paying attention to the restoration of its congruence. The macroscopic evaluation standards of the International Cartilage Restoration Society (ICRS)

**The aim of our study** was to investigate the safety and efficiency of the application of a biodegradable implant produced from polycaprolactone with the method of electrospinning and coated with hydroxyapatite and its impact on healing of an intra-articular defect in the loaded zone of the knee joint in rats.

were used [23]. The ICRS macroscopic evaluation of osteochondral repair has been widely used to study the repair of an osteochondral defect *in vivo* [24, 25, 26]. Two orthopedic surgeons and a histology researcher performed a blind evaluation of the effect of defect repair. Photographic digital documentation of anatomical preparations was carried out.

### *Biomechanical methods*

To analyze the biomechanical properties of the articular surface of the regenerate formed in the area of the osteochondral defect, its compliance (P) was determined on fresh unfixed anatomical preparations (measuring the magnitude of the applied force as a result of the forced introduction of the indenter into the tissue under study). To do this, we used a pointer indicator with measurement steps from 0 to 10 mm and a division value of 0.01 mm (GOST 577-68) with a spherical shape of the indenter. The curvature of the cartilaginous surface was determined by a radius meter in the radius range of 0.5-10 mm. The measurements were performed as follows: the curvature of the cartilaginous surface was measured with a radius meter, setting the measuring device on a template corresponding to the radius of the cartilage surface curvature (the steady indicator reading is Mo), similarly, the value of penetration of the indenter into the cartilage was measured (M – according to the indication of the indicator arrow). The contact time of the indenter with the cartilage was 3-5 seconds. Each of the measurements was repeated three times. Average values were calculated. According to the formula  $P = 10.5 M + 70$  (where P is the force of the spring mechanism, measured in gram-force (gf)) were determined the magnitude of the force P, with which the movable leg of the device penetrated into the cartilage.

Having determined the value of the indenter penetration (d) (in accordance with the readings of the digital indicator, where  $d = Mo - M$ ), the compliance (P) was calculated:  $P = d/P$  in mm/gf, given that  $1 \text{ m/N} = 0.102 \text{ mm/gf}$ .

### *Histological methods*

Fragments of the distal articular end of the femur dissected from soft tissues were fixed in 10 % neutral formalin solution for 3-5 days. Samples were demineralized in a decalcifying solution based on EDTA by constant shaking and changing solutions every day for 7-10 days. For dehydration of bone and cartilage

fragments, alcohols of ascending strength (from 70° to 100°) were used. The samples were then impregnated and embedded in paraffin.

Histological sections, 5-7 µm thick, were prepared using a sledge microtome (Reichert, Germany), placed on glass slides and dried. Deparaffinized preparations were stained with hematoxylin and eosin, as well as alcian blue – safranin-O. An immunohistochemical reaction to CD34 antibodies was carried out by additional staining with hematoxylin and eosin (protocol and antibodies from Abcam PLC, UK).

Light microscopic study and digitization of histological preparations were performed using an AxioLab.A1 microscope and an AxioCam digital camera (Carl Zeiss MicroImaging GmbH, Germany). The thickness of the subchondral bone trabeculae was measured with VideoTesT Master-Morphology-4.0 (NPK Zenit Ltd, Russia). The thickness of the cartilage tissue in the defect zone was measured after 180 and 360 days on digitized images of histological preparations of the experiment series and intact animals. The areas of tissue components in the regenerate formed

in the defect zone were measured and their portion in the total area of the regenerate at different time-points of the experiment was calculated. Blind histological assessment was carried out according to the system proposed by O'Driscoll et al [27].

#### Statistical methods

Statistical analysis was performed using Attestat software 9.3.1. The values were presented as medians (Me) and quartiles (Q1-Q3). The significance of differences was determined by the Mann-Whitney test. At  $p < 0.05$ , the differences were considered statistically significant.

Ethics Approval was obtained from the institutional ethics committee before the experiment (Ethics Committee of the Ilizarov National Medical Research Center for Traumatology and Orthopedics, Kurgan, Russia(protocolcode 1(71),date of approval 28.04.2022). Interventions, animal care, and euthanasia conformed to the requirements of the European Convention for the Protection of Vertebrate Animals used for Experimental and other Scientific Purposes (Strasbourg, 18.03.1986), principles of laboratory animal care (NIH publication number 85-23, revised 1985), and the national laws.

## RESULTS

### Clinical assessment

After 14 days, the rats actively used the involved limb. Their behavior, food intake and physical activity did not differ from intact animals. Tissue swelling persisted for 7 days post-surgery. Measurements of the circumference of the upper third of the leg showed slightly lower volume of soft tissues of involved limbs in the control group in comparison to the experimental group (Fig. 1).

Neither weight loss nor critical changes in the body temperature were observed in the animals of both groups (Table 1). There was a slight increase in body temperature within 30 days after surgery in both groups. The local temperature in the joint area within a month after surgery was higher than the reference values by 2.6-2.7 °C in both groups.

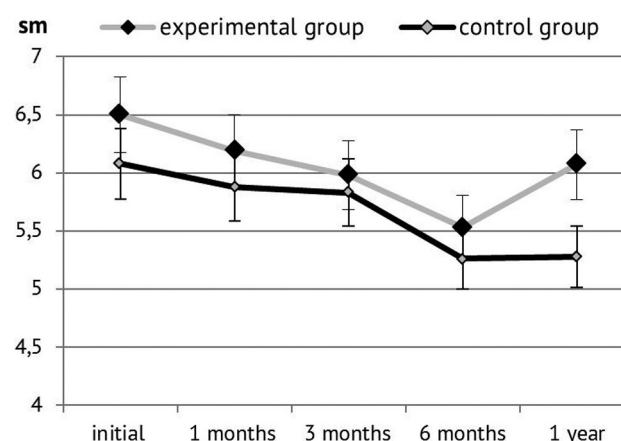


Fig. 1 Soft tissue circumference of the lower leg

Physiological parameters: weight, local and body temperature

Table 1

Experiment time-point	Animal group	Parameters		
		Body weight [gr]	General body temperature [°C]	Local temperature [°C]
Reference norm	—	397.0 (342-406)	34.6 (34.5-35.1)	31.1 (30.1-31.8)
14 days	Control	402.3 (331-409)	36.9 (36.4-36.9)*	33.7 (31.0-33.5) *
	Experiment	403.8 (344-409)	37 (36.7-36.9) *	33.8 (32.4-33.8) *
30 days	Control	408 (328-410)	36.2 (36.1-36.4) *	32.2 (31.2-32.2)
	Experiment	408 (344-416)	36.4 (35.8-36.5) *	31.2 (30-31.4)
60 days	Control	408.4 (343-412)	35.1 (34.7-35.4)	28.8 (28.5-28.9) *
	Experiment	409.0 (348-419)	35.6 (34.7-35.5)	31.1 (30.4-31.5)
90 days	Control	410.0 (338-410)	34.9 (33.5-35.05)	30.2 (28.85-31.2)*
	Experiment	410.0 (350-434)	35.03 (34.4-35.1)	31.3 (30.8-31.3)
180 days	Control	393(391-395)	35.1 (34.9-35.3)	30.8 (29.8-31.8)
	Experiment	413 (411-415)	34.9 (34.7-35.1)	30.7 (30.1-31.8)
360 days	Control	401 (398-404)	35.6 (35.5-35.7)*	30.4(29.7-31)*
	Experiment	418 (410-426)	35.1 (34.9-35.3)	30.9(30.4-31.4)

\* significant difference,  $p < 0.05$

At any time-point of the study, range of knee motion in experimental and control animals did not significantly differed from each other and from intact rats (Fig. 2). But at the 1-year point, the values of knee extension in both groups were reduced relative to the previous measurements by 8.1 % in the experimental group and by 16.5 % in the control group. At the same time, in the experimental group, the values did not have significant differences from intact animals and were higher than in the control group by 11 %.

Knee flexion values in both groups did not differ from those in intact animals. However, a slight decrease was noted after 30 days in both groups (by 3 % and by 1.5 %, in the experimental and control groups, respectively) and after a year in the control group (by 1.5 %). At the same time, from 90 days to 360 days, the indicators of the experimental group exceeded those in the control one by 2 %-2.9 %. So, there was no significant difference in ROM between the groups.

#### Results of anatomical and histological study

The study of anatomical preparations of the distal articular end of the femur showed that in the animals of the experimental group, a smooth shiny articular surface was seen and preservation of the anatomical relief of the condyle already after 14 days due to the implanted material filling the defect gap. The defect was covered with a layer of transparent tissue under which the implant material was visualized filling the defect (Fig. 3 i). There were no signs of implant rejection, inflammatory reaction of surrounding tissues and cavities around it. On day 60, the layer of tissue on the implant surface was more pronounced, and the surface congruence was maintained (Fig. 3 j). throughout the study including long-term, the anatomical relief of the surface in the area of damage was preserved in experimental group (Fig. 3 k, l). Visualization of the implant at each subsequent study time-point was less expressed (Fig. 3 j, k, l). At six months post-surgery, the defect site was

completely replaced by specific tissues. The lateral femoral condyle retained its anatomical shape without erosion. The color and gloss of the surface was similar to the norm (Fig. 3 l).

In the control group, the bottom of the defect was lined with a smooth tissue layer in all periods, denser and less transparent along the perimeter of the edge of the defect (Fig. 3 a-d). However, the defect was not filled even after 180 days of the experiment (Fig. 3 c). After 360 days, the defect was unevenly filled with a connective tissue substrate (Fig. 3 d). The congruity of the surface was disturbed at all time-points of the experiment (Fig. 3 a-d). In the intact lateral condyle, areas with erosions on the cartilage surface were visualized starting from day 60 of the experiment (Fig. 3 b, c, d).

At all time-points of the experiment, the indicators of macroscopic assessment according to the ICRS standards in the experimental group were significantly higher than in the control group (Table 2). The maximum scores were noted in the experimental group after six months and a year of the experiment. By those time-points, cartilage recovery was close to normal and corresponded to the grade II of healing while in the control group, the result corresponded to grades III and IV, which are characterized as abnormal and extremely abnormal recovery. The results obtained are consistent with those of descriptive morphology.

Table 2

Results of macroscopic study of osteochondral defect recovery (ICRS standards)

Group	Number of points, Me (Q1-Q3)		
	60 days	180 days	360 days
Control	2.5 (2.3-2.6)*	4 (3.9-4.2)*	4.5 (4.3-4.7)*
Experimental	10 (9.5-10.5)	10.5 (10.3-10.7)	11 (10.8-11.4)

\*significant difference ( $p < 0.01$ )

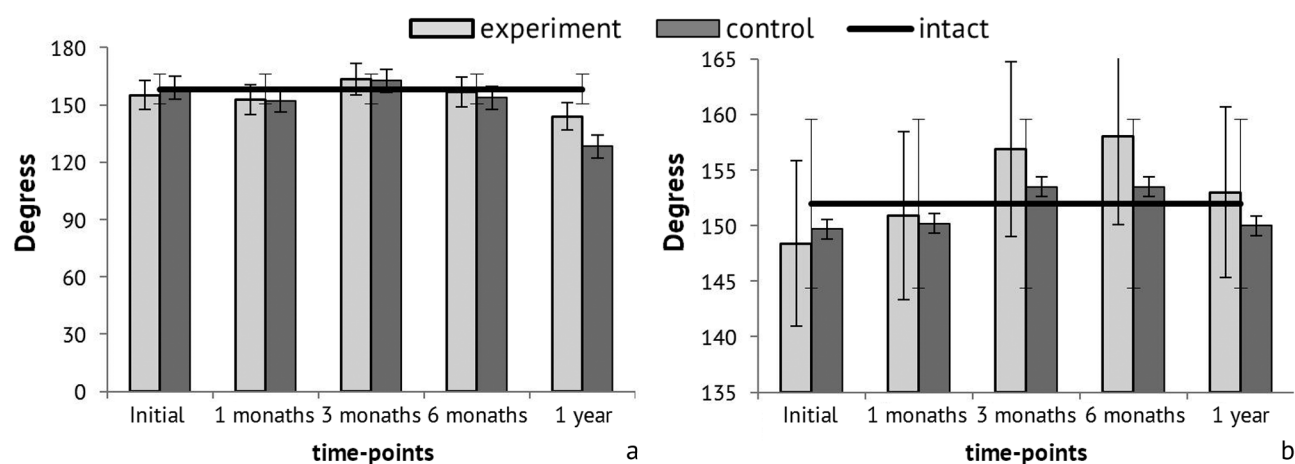
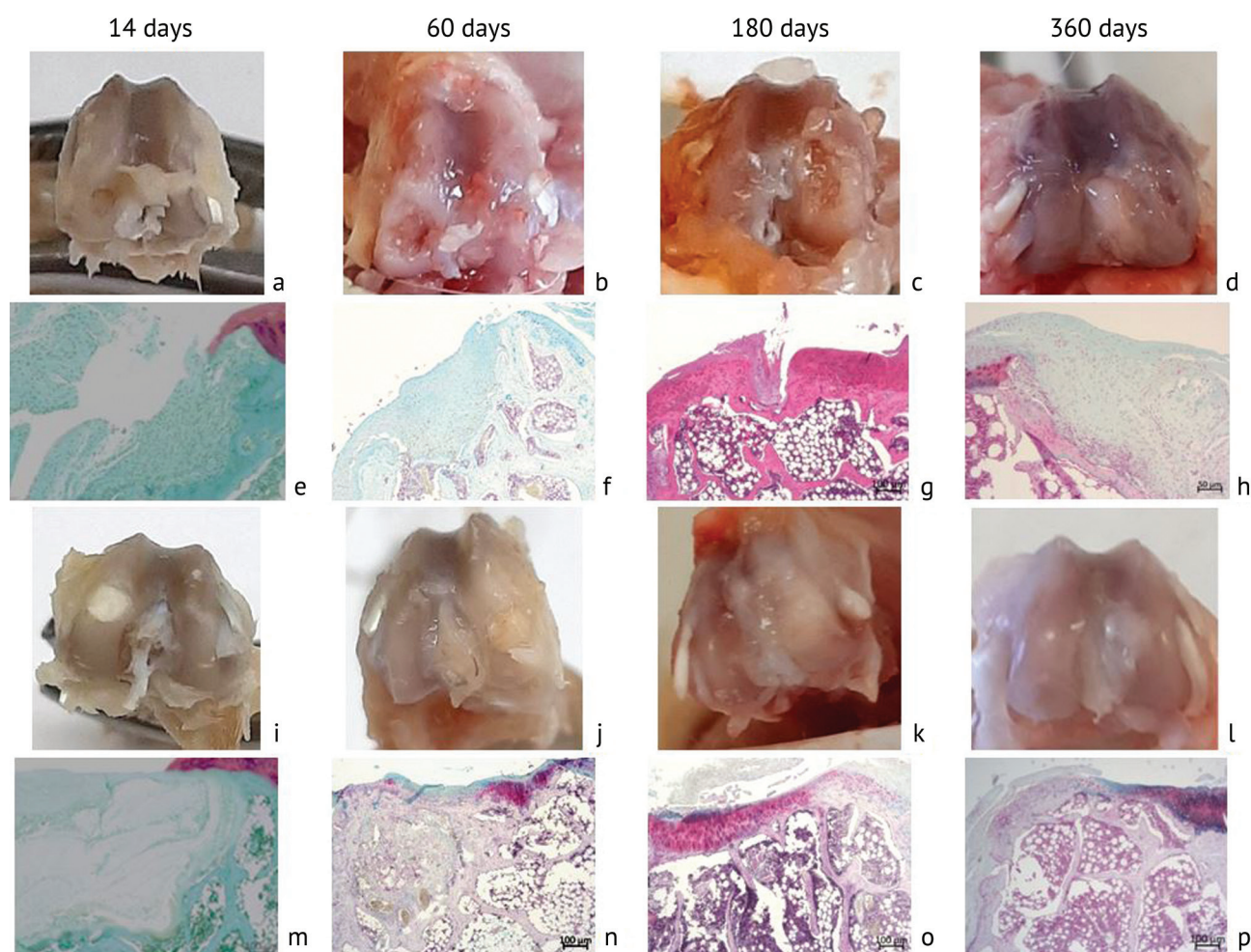


Fig. 2 Range of motion in knee joint: a – extension, b – flexion





**Fig. 3** Anatomical and histotopographic macro- and microphotos of the osteochondral defect at different time-points of the experiment. Anatomical preparations of the distal articular end of the femur in the control group (a-d); histotopographic sections of the area of the osteochondral defect of the femoral condyle in the control group (e-h); anatomical preparations of the distal articular end of the femur in the experimental group (i-l); histotopographic sections of the area of osteochondral defect of the femoral condyle in the experimental group (m-p); f, g, h, p – Staining with hematoxylin and eosin (e, f, g, m); alcian blue-safranin staining (h, n, o, p). Magnification (e-h, m-p):50×

Histological methods showed that the area of the defect in the experimental group was densely filled with implant material after 14 days, around which granulation and loose fibrous connective tissue and microvessels were detected (Fig. 3 m). Bands of loose fibrous connective tissue containing microvessels, an accumulation of poorly differentiated fibroblast-like cells, cells of the monocyte-macrophage series and lymphocytes grew from the side of the surrounding subchondral bone into the spaces between the structures of the implant (Fig. 4 b). Among them, there were cells in a state of division (Fig. 4 c). Inflammatory infiltrates around the structures of the implant material were not observed. In the intertrabecular spaces of the subchondral bone adjacent to the defect, predominantly red (hematopoietic) bone marrow was seen. Outside, small areas of hyaline-like cartilage crawled onto the implant filling the defect from the side of the preserved hyaline cartilage, connected with avascular fibrous connective tissue with small areas of granulations, covering most of the surface of the defect (Fig. 3 m, Fig. 4 a).

In the control group, the defect was predominantly filled with loose fibrous tissue with granulation foci (Fig. 3 e, Fig. 4 d, e). In the intertrabecular spaces, inflammatory infiltrates, loose fibrous connective tissue, and foci of hematopoiesis were noted (Fig. 4 e).

After 60 days of the experiment, the volume of the implant material significantly decreased due to its biodegradation and replacement with tissue components; in the projection of the subchondral bone with reticulofibrous bone and loose fibrous connective tissues with numerous microvessels, and in the projection of the cartilaginous lining from the side of intact hyaline cartilage with small foci of hyaline-like tissue, and in the middle part with fibrocartilaginous tissue (Fig. 5 a).

Bone trabeculae along the periphery of the defect area were more mature and mineralized but slightly mineralized in the middle part (Fig. 5 c). The cell composition was characterized by cells of epithelial, fibroblastic, osteogenic and monocyte-macrophage differons. Osteoclasts were determined (Fig. 5 d).



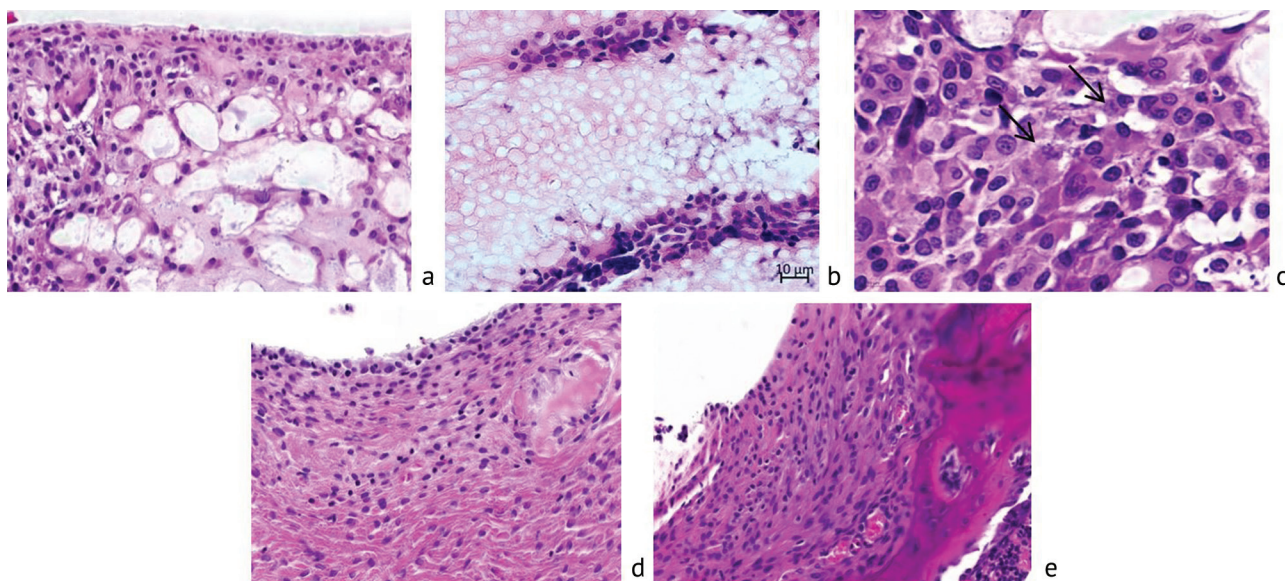


**Fig. 4** Features of the regenerate in the area of the osteochondral defect after 14 days of the experiment. Experimental group: articular surface in the area of the defect replaced by the implant (a); ingrowth of loose fibrous connective tissue into the structure of the implant (b); (c) mitotically dividing cells in the regenerate formed in the area of the osteochondral defect (arrows). Control group: articular surface in the area of the defect (d); loose fibrous connective tissue that fills the defect and trabecular subchondral bone that forms the bed of the defect (e). Staining with hematoxylin and eosin. Magnification: a, b, d, e – 400×; c – 1000×

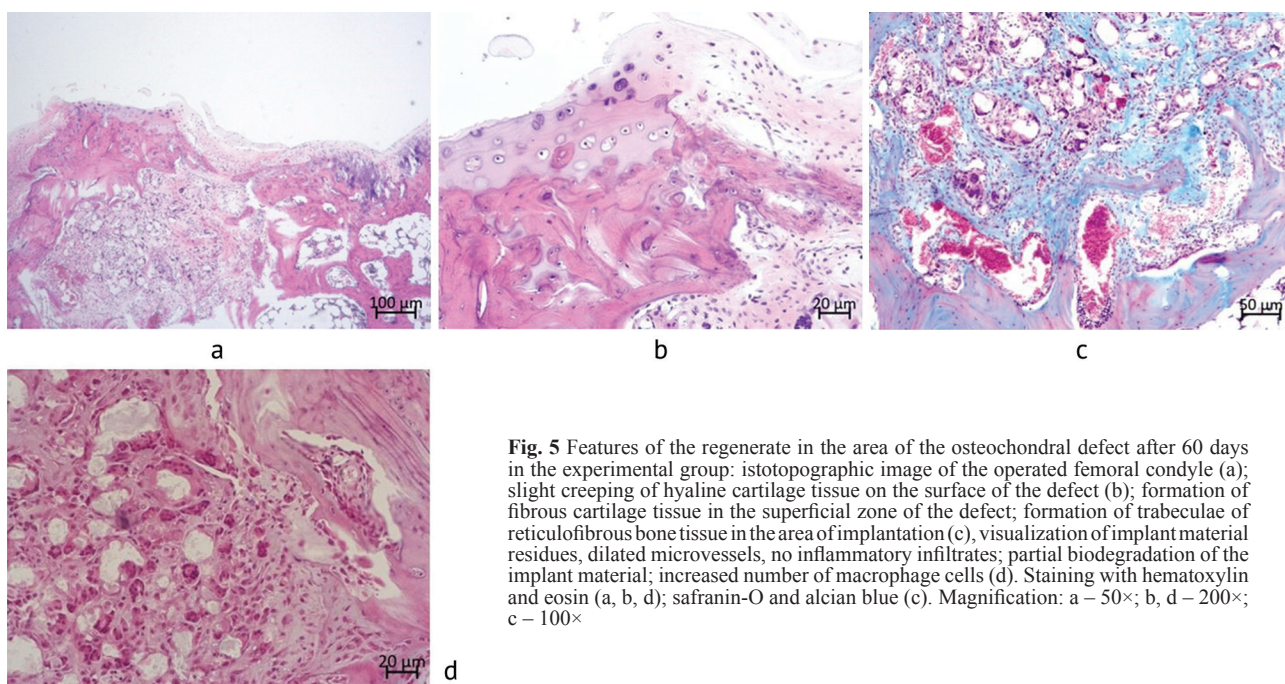


**Fig. 5** Features of the regenerate in the area of the osteochondral defect after 60 days in the experimental group: isotopographic image of the operated femoral condyle (a); slight creeping of hyaline cartilage tissue on the surface of the defect (b); formation of fibrous cartilage tissue in the superficial zone of the defect; formation of trabeculae of reticulofibrous bone tissue in the area of implantation (c); visualization of implant material residues, dilated microvessels, no inflammatory infiltrates; partial biodegradation of the implant material; increased number of macrophage cells (d). Staining with hematoxylin and eosin (a, b, d); safranin-O and alcian blue (c). Magnification: a – 50×; b, d – 200×; c – 100×

Giant cells of foreign bodies were not found. Microvessels in the area of the defect and adjacent parts of the subchondral bone were plethoric and dilated. In the projection of the cartilage, the vessels were not found. There was no rarefaction of the subchondral bone beyond the defect area. Vessels and hematopoietic-fatty bone marrow were visualized in the intertrabecular spaces.

In the control group after 60 days, the defect was partially covered by the trabecular bone from the side of the subchondral bone (Fig. 6 a) and with fibrous tissue in the central part (Fig. 6 a, b). Surface congruence was not achieved and a crescent cavity

was noted (Fig. 3 b, f, Fig. 6 a). From the side of the cartilage lining, no creeping of hyaline cartilage tissue into the defect area was detected (Fig. 6 b). The vessels in the intertrabecular spaces were dilated. Lymphocytic infiltrates were determined along their periphery (Fig. 6 c). A thickening of the subchondral compact plate was noted at the edges of the defect (Fig. 6 b). The bone marrow in the intertrabecular spaces was predominantly hematopoietic-fatty.

After 180 days in the experimental and control series the subchondral defect was replaced by trabecular bone of hematopoietic-fatty marrow in the intertrabecular spaces (Fig. 3 o, g, Fig. 7 a, c, Fig. 8 a, d).



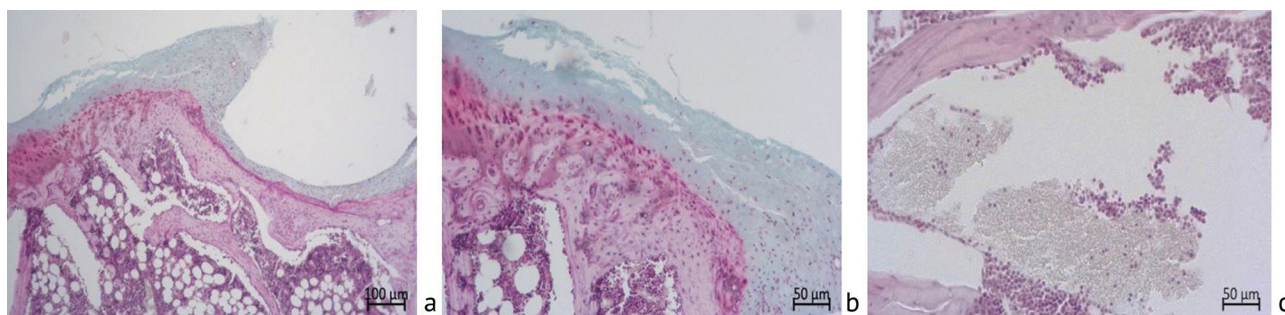


**Fig. 6** Features of the regenerate in the area of the osteochondral defect after 60 days of the experiment. Control group: histotopographic image of the operated femoral condyle (a); thickening of the compact plate of the subchondral bone at the edges of the defect (b) and filling the defect with fibrous connective tissue; dilated sinusoidal capillaries with lymphocytic infiltrate in the perivascular region (c). Staining: safranin-O and alcian blue. Magnification: a – 50×; b, c – 100×

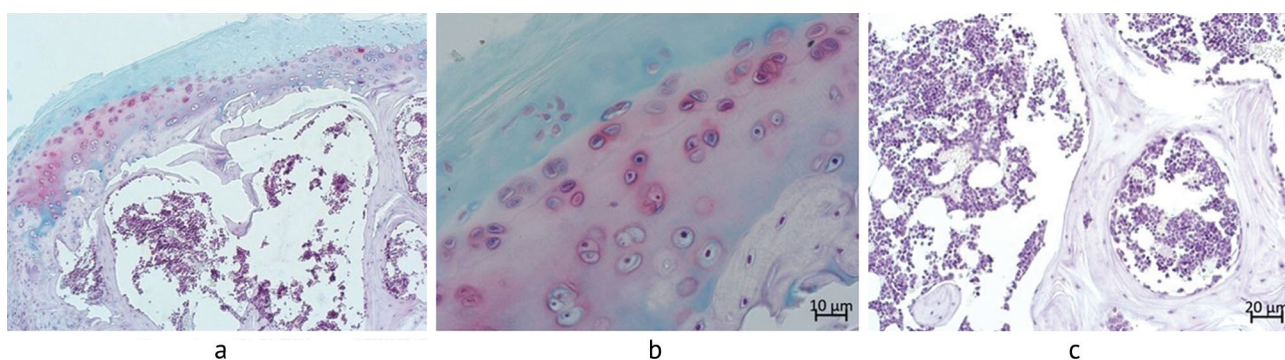


**Fig. 7** Features of the regenerate in the area of the osteochondral defect after 180 days of the experiment. Experienced group: formation of a cartilaginous lining throughout the replaced osteochondral defect (a); zonal structure of the newly formed hyaline cartilage, fibrillation of the outer zone, the appearance of isogenic groups of young chondrocytes in the median zone, a volumetric zone of calcified cartilage (b); hematopoietic bone marrow with fat cells in the intertrabecular spaces of the replaced area of the subchondral bone in the area of the defect (c); a fragment of the implant material embedded in the structure of the bone trabecula (d). Staining: a-d – safranin-O and alcian blue. Magnification: a – 50×; c – 100×; b, d – 200×

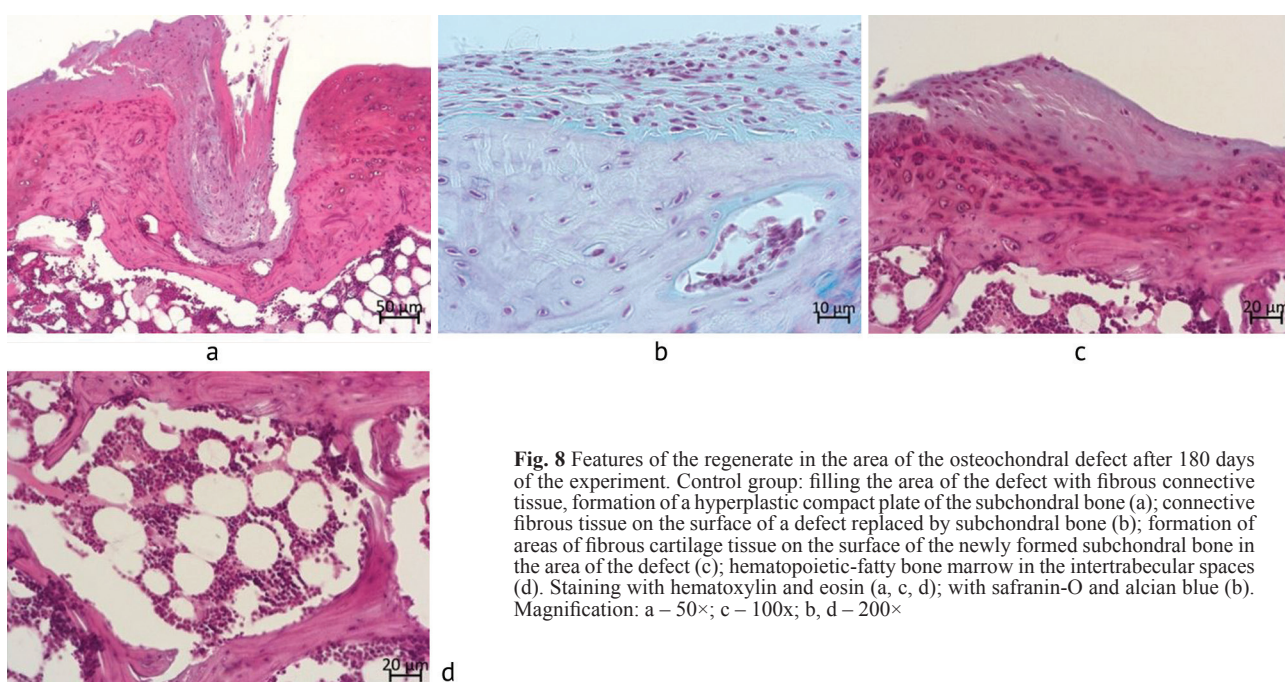


**Fig. 8** Features of the regenerate in the area of the osteochondral defect after 180 days of the experiment. Control group: filling the area of the defect with fibrous connective tissue, formation of a hyperplastic compact plate of the subchondral bone (a); connective fibrous tissue on the surface of a defect replaced by subchondral bone (b); formation of areas of fibrous cartilage tissue on the surface of the newly formed subchondral bone in the area of the defect (c); hematopoietic-fatty bone marrow in the intertrabecular spaces (d). Staining: a, c, d – hematoxylin and eosin; b – safranin-O and alcian blue. Magnification: a – 50×; c – 100×; b, d – 200×



In the control group, compacted bone conglomerates were formed closer to the outer surface of the condyle, similar to osteophytes (Fig. 3 g). In the projection of the articular cartilage, the area of the defect in the experimental series was replaced by a layer of hyaline cartilage tissue (Fig. 3 o, Fig. 7 a, b) while in the control group by a layer of fibrous connective tissue (Fig. 3 g; Fig. 8 a, b), in a separate case in combination with small fragments of fibrous connective tissue (Fig. 8 c). The remnants of the implant material in the area of the defect in the animals of the experimental series were not found what indicated its complete biodegradation by this period. In one field of vision, there was an area with a small fragment of the implant material embedded in the structure of bone trabecula (Fig. 7 d).

Immunohistochemical staining for CD 34 revealed newly formed vessels in the superficial

connective tissue layer in control animals (Fig. 9 b). In the experimental group in the newly formed cartilage tissue formed in the area of the defect, the test was negative (Fig. 9 a).

After a year in the experimental group, the preservation of the integrity of the cartilage lining was noted. The newly formed cartilage acquired a zonal structure. It contained superficial (more voluminous than in intact animals), intermediate with small isogenic groups, and deep zones (Fig. 3 a, Fig. 10 a). In the control animals, the superficial area of the defect was filled with fibrous tissue, sometimes with small areas of fibrous cartilage (Fig. 3 h, Fig. 10 b). The subchondral bone in the experimental group practically did not differ from that in intact animals (Fig. 3 p, Fig. 10 d, f). In the controls, it was slightly sparse, with a thickened compact plate in the area of the defect (Fig. 3 h, Fig. 10 e).

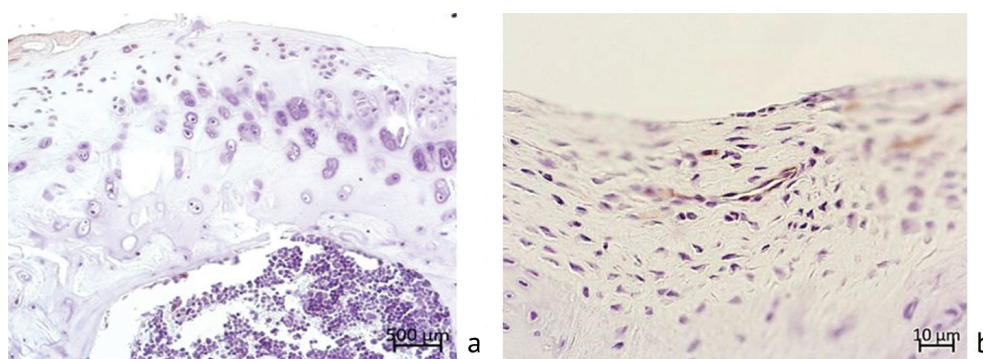


**Fig. 9** Immunohistochemical staining to detect vessels in the surface lining of the regenerate of an osteochondral defect; vessels were not identified in the experimental group (a); microvessels were detected in the control group (b, brown staining). Staining is an immunohistochemical reaction using antibodies to CD34. Magnification – 400×

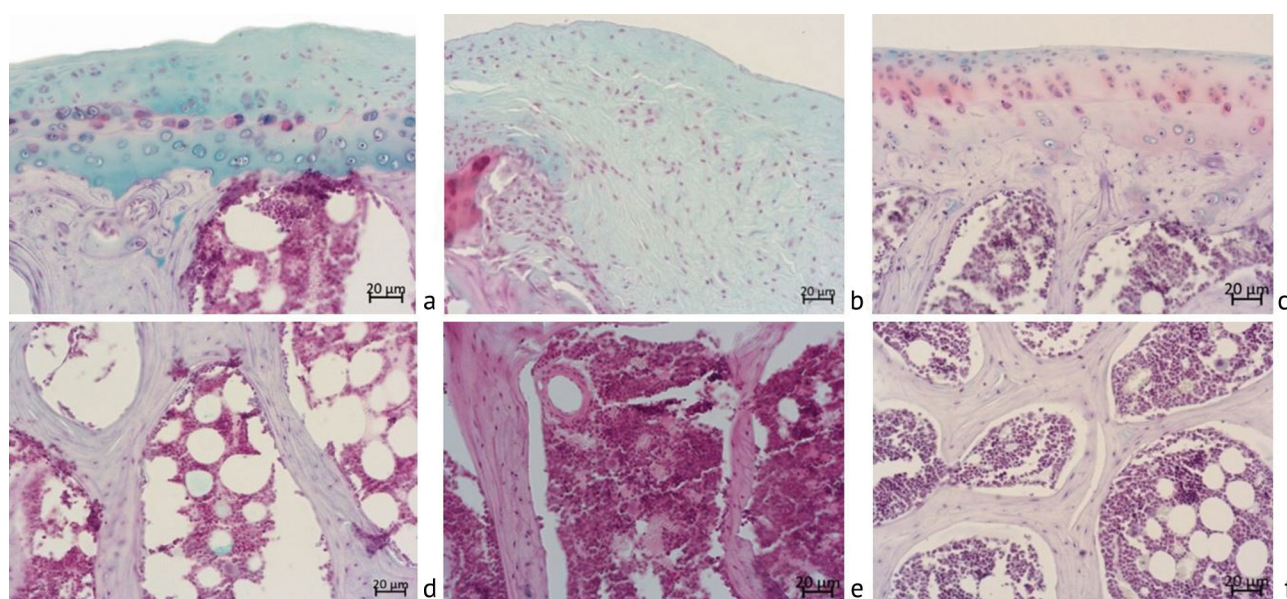


**Fig. 10** Regenerate features in the subchondral defect area after 360 days of the experiment: a – formation of hyaline cartilage tissue of zonal structure in the experimental group; b – filling the defect area with fibrous connective tissue in the control group; c – structure of the articular cartilage in intact animals of the same age; d-f – structure of subchondral bone (d – experimental group, e – control group, f – intact animals). Staining: a-e – safranin-O and alcian blue. Magnification: a-e – 200×



A semi-quantitative assessment of the completeness of replacement and recovery of tissues in the area of the osteochondral defect showed that in all periods of the experiment, a more complete recovery was observed in the experimental group (Table 3). After 60 days, the median of the experimental group was 1.7 times higher than that in the control group, after 180 days by 3.12 times, after a year of the experiment by 3.25 times. Since the maximum number of points for this assessment system is 28 points, it can be said that after 180 days the healing of the articular surface defect in the experimental group was almost complete, and after a year of the experiment it was complete. In the control group, the healing of the defect was very poor even after a year.

The analysis of morphometric data showed significant differences in the fractional components of the tissue components of the regenerate in the defect area in the experimental and control groups in almost all periods of the experiment (Table 4). In the control series,

there was no implant material and in none of the periods was the formation of hyaline cartilage tissue detected. Its fraction in the total structure of the regenerate was equal to zero. However, the fractions of bone tissue and bone marrow in the regenerates of the control and experimental groups did not have significant differences after 2 months and after 1 year of the experiment.

Table 3  
Results of a semi-quantitative histological assessment of the completeness of osteochondral defect filling according to O'Driscoll (modified)

Group	Number of points at experiment time-points, Me (Q1-Q3)		
	60 days	180 days	360 days
Controls	4.4 (4.2-4.6)	7.5 (6.7-8.2)	8 (7.7-8.3)
Experimental	7.6 (7.3-8.1)	23.4 (23.3-23.7)	26 (25.8-27.3)

Notes: the maximum possible number of points is 28;  
p < 0.01 – differences between the groups are significant at all time-points

Table 4  
Fractions of tissue components in the regenerate filling the osteochondral defect

Experiment time-point	Series	Fractions of tissue components (%). Me (Q1-Q3)					
		Bone marrow	Bone tissue	Fibrous connective tissue	Fibrous cartilage tissue	Hyaline cartilage	Implanted material
14 days	Control	0 <sup>2</sup> p = 4.26E-0.5	9.9 (8.7-11.1) <sup>1</sup> p = 0.035 <sup>2</sup> p = 0.008	90.1 (88.3-91.9) <sup>1</sup> p = 5.85E-07 <sup>2</sup> p = 0.0006	0 <sup>1</sup> p = 0.011	0 <sup>2</sup> p = 0.011	0 <sup>1</sup> p = 0.00018 <sup>3</sup> p = 0.000182
	Experimental	0 <sup>2</sup> p = 4.26E-0.5	6.2 (5.9-6.5) <sup>1</sup> p = 0.035 <sup>2</sup> p = 0.056	13.5 (11.2-14.1) <sup>1</sup> p = 5.85E-07 <sup>2</sup> p = 0.004	3.2 (2.6-3.8) <sup>1</sup> p = 0.011 <sup>2</sup> p = 0.004	0 <sup>2</sup> p = 0.011	77.1 (75.3-78.9) <sup>1</sup> p = 0.00018 <sup>2</sup> p = 2.5E-07
2 months	Control	24.6 (23.3-27.1) <sup>1</sup> p = <b>0.11</b> <sup>2</sup> p = 0.016 <sup>3</sup> p = 0.019	43 (42-47) <sup>1</sup> p = <b>0.78</b> <sup>2</sup> p = 0.027 <sup>3</sup> p = 0.00026	28 (24.7-30) <sup>1</sup> p = 0.0023 <sup>3</sup> p = 0.00026	0 <sup>1</sup> p = 0.0014 <sup>2</sup> p = 0.031 <sup>3</sup> p = 4.69E-0.6	0 <sup>1</sup> p = 0.0017 <sup>2</sup> p = 0.011 <sup>3</sup> p = 4.69E-0.6	0 <sup>1</sup> p = 0.0014
	Experimental	21.7 (21.3-22.2) <sup>1</sup> p = <b>0.11</b> <sup>3</sup> p = 0.017	44.1 (43.7-45.7) <sup>1</sup> p = <b>0.78</b> <sup>3</sup> p = 0.00027	21 (43.7-45.7) <sup>1</sup> p = 0.0023 <sup>3</sup> p = 0.003	2.8 (2.5-3.3) <sup>1</sup> p = 0.0014 <sup>3</sup> p = <b>0.43</b>	3.5 (3.4-3.7) <sup>1</sup> p = 0.0017 <sup>3</sup> p = 0.0016	6.1 (7.1-5.6) <sup>1</sup> p = 0.0014 <sup>3</sup> p = 0.0002
6 months	Control	29.2 (28.9-33) <sup>1</sup> p = 0.08 <sup>2</sup> p = 0.0033 <sup>3</sup> p = 0.035	57.2 (53.7-62.7) <sup>1</sup> p = 0.008 <sup>2</sup> p = 0.0025 <sup>3</sup> p = 0.02	8.1 (7.4-9.9) <sup>1</sup> p = 0.013 <sup>2</sup> p = 0.0084 <sup>3</sup> p = 0.0016	<b>0.68 (0.51-1.74)</b> <sup>1</sup> p = 0.013 <sup>2</sup> p = 0.0084 <sup>3</sup> p = 0.0015	0 <sup>1</sup> p = 0.08 <sup>2</sup> p = 0.0015	0 <sup>1</sup> p = <b>0.42</b>
	Experimental	45.1 (44.5-45.3) <sup>1</sup> p = 0.08 <sup>2</sup> p = 3.18E-0.5 <sup>3</sup> p = 4.06E-07	38 (36-45) <sup>1</sup> p = 0.008 <sup>2</sup> p = <b>0.24</b> <sup>3</sup> p = <b>0.22</b>	5.9 (5.7-6.1) <sup>1</sup> p = 0.013 <sup>2</sup> p = 0.000025 <sup>3</sup> p = 2.98E-0.5	0 <sup>1</sup> p = 0.013 <sup>3</sup> p = 0.007	9.6 (3.8-13.1) <sup>1</sup> p = 0.08 <sup>2</sup> p = <b>0.63</b> <sup>3</sup> p = 0.043	0.46 (0.36-1.38) <sup>1</sup> p = <b>0.42</b> <sup>2</sup> p = <b>0.42</b> <sup>3</sup> p = 0.022
1 year	Control	39.8 (36-50.7) <sup>1</sup> p = <b>0.16</b> <sup>2</sup> p = <b>0.165</b> <sup>3</sup> p = <b>0.12</b>	34 (33-39.1) <sup>1</sup> p = <b>0.31</b> <sup>2</sup> p = <b>0.45</b> <sup>3</sup> p = <b>0.78</b>	26.4 (10-40.4) <sup>1</sup> p = <b>0.1</b> <sup>2</sup> p = 0.01 <sup>3</sup> p = <b>0.19</b>	0 <sup>3</sup> p = 0.013	0 <sup>1</sup> p = 0.02 <sup>2</sup> p = 0.0015	0
	Experimental	52.7 (46.71-54.43) <sup>1</sup> p = <b>0.16</b> <sup>2</sup> p = <b>0.398</b> <sup>3</sup> p = 3.18E-05	30.28 (16.58-32.3) <sup>1</sup> p = <b>0.1</b> <sup>2</sup> p = <b>0.21</b> <sup>3</sup> p = 0.247	0 <sup>1</sup> p = <b>0.1</b>	0	12.86 (9.07-16.65) <sup>1</sup> p = 0.02 <sup>2</sup> p = <b>0.17</b> <sup>3</sup> p = 0.63	0 <sup>3</sup> p = 0.022
Intact		54.1 (53.1-54.2)	36.8 (30.63-37.43)	0	0	10.4 (9-12.6)	0

Notes: <sup>1</sup>p – significance of differences between the groups; <sup>2</sup>p – significance of difference compared with experimental animals; <sup>3</sup>p – significance of difference as compared with the previous experimental time-point. Differences are significant at p < 0.05; **bold typed** are values that do not have significant difference (p > 0.05)

The content of connective tissue in regenerates filling osteochondral defects in animals of the control group was significantly higher than in the experimental group: after 14 days by 95 %, after 60 days – by 25 %, after 180 days – by 27.2 %, and after 360 days – by 73.6 %. In both groups, the maximum content of fibrous connective tissue in the composition of the regenerate was observed by day 60. By day 180, this component decreased by 71-72 % in both groups, while in the experimental group its portion was very small, only 5.9 %. After a year of the experiment, there was no fibrous connective tissue in the regenerate of the experimental group animals. In the control group, it occupied almost one third of the regenerate. Hyaline cartilage tissue in the experimental group was detected after 60 days of the experiment. Its content significantly increased by 36.5 % after 180 days of the experiment, and by another 25.3 % after a year (360 days). The content in those periods corresponded much to the indicators in the intact rats. After 360 days of the experiment, the regenerates of the experimental group animals contained only bone tissue, bone marrow and hyaline cartilage tissue. Their fractional content was similar to that in intact animals.

In the control group, the content of bone tissue and bone marrow did not have significant differences from the experimental and intact groups at that time-point. At the same time, the portion of fibrous connective tissue was about 30 %, and the hyaline tissue was absent. The content of the implant material in the experimental group significantly reduced as the experiment period increased. Within the time points of 14 to 60 days, its content decreased by 92 %. By day 180 of the experiment, there was no implant material in the regenerate in the area of the osteochondral defect. It completely degraded by that time-point. The thickness of the cartilaginous lining in the area of the osteochondral defect after 180 days was significantly higher than that in the norm (Fig. 11). A year later, the thickness of the articular cartilage was comparable to that in intact animals of the same age. Morphometry of the subchondral bone trabeculae thickness showed that they were thicker in the experimental group than in the control group. Their thickness after a year did not differ from that in intact rats (Fig. 12).

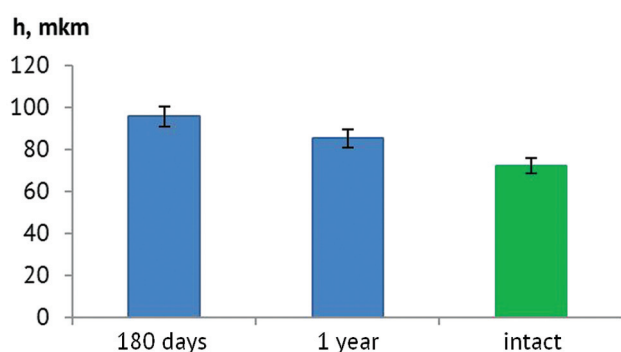


Fig. 11 Thickness of the articular cartilage in the experiment group after 180 days and a year relative the intact animals

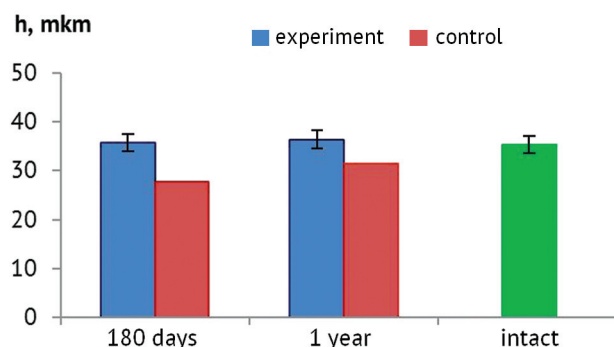


Fig. 12 Thickness of the subchondral bone trabeculae in the area of the osteochondral defect after six months and in a year of the study

### Biomechanical study

Biomechanical methods established that the values of regenerate compliance in the area of the osteochondral defect relative to the control group were reduced by 29.2 % and by 18.5 % in the experiment group by day 60 of the experiment, but did not have significant difference compared to similar indicators in intact animals (Table 5). The values of the experimental group exceeded those in the control group by 15 %. After 180 days of the experiment, the biomechanical properties increased in both series: insignificantly in the control group by only 3 %, and by 11.9 % in the experimental group. In the experimental group, the values did not significantly differ from those in intact animals; in the control they remained lower by 26.2 %.

Table 5

Biomechanical properties of the regenerated articular surface in the osteochondral defect

Experiment time-point (days)	P – compliance, 10 mm <sup>3</sup> /g*cm	
	Control group	Experimental group
60 days	1.956 (1.597-1.982)*	2.250 (2.167-2.628) #
180 days	2.009 (1.580-2.250)*	2.553 (1.607-2.727)
360 days	1.997 (1.898-2.210)*	2.599 (2.408-2.691)#
Intact	2.762 (2.221-2.978)	

\* –  $p < 0.05$  – significant difference with intact animals;  
# –  $p < 0.05$  significant difference with the control group.

After 360 days, the values of compliance of the regenerate formed in the area of the osteochondral defect did not differ from the previous period in the experimental group. In the experimental group, they slightly increased by 2 %, while in the control group they decreased by 1 %. As in the previous time-point, the animals of the experimental group did not show significant differences in the values of articular surface compliance from those in the intact animals while in the control animals they were significantly lower (by 27.2 %).

The study showed that the mechanical properties of the cartilage recovered to the level of the intact animals by day 60 in the experimental group and persisted up to 360 days, while in the control group they did not recover even after 360 days.



## DISCUSSION

A lot of researchers worldwide have been searching for the ways to solve the problem of treating irreparable osteochondral defects. Many options have been proposed, including those using bioengineering technologies [30]. However, a perfect method of tissue repair in the area of an osteochondral defect, the effect of which could be preserved for a long period, has not been developed so far [18]. Therefore, the search for the ways to successfully manage irreparable articular surface defects continues and is aimed at prevention or delay of joint replacement procedures. The greatest preference would be given to less expensive and one-step techniques [17].

Previously, it was found that the most effective regeneration of hyaline-like cartilage is possible only with the use of collagen matrices populated with autologous cartilage cells in combination with microfracturing [31]. There are data on the positive use of cell-free collagen scaffolds [32, 33]. Some studies have shown that collagen matrices did not contribute to the restoration of joint surface congruence [34].

An alternative to collagen matrices has recently been polymeric implants. Polycaprolactone (PLC) is one of the most commonly used polymers in tissue engineering to restore the loss of bone and cartilage tissue [26, 35, 36]. One of its shortcomings is its low adhesive ability [37]. Many authors compensate for this drawback by adding hydroxyapatite particles to its composition or apply them to the surface of PLC products. Thus, this composite biomaterial has induction properties, is able to enhance proliferation and have effect on cell differentiation [38, 39].

It is known that the hydroxyapatite nanocomposite has greater biocompatibility and better adhesion properties of its surface compared to the microcomposite [40, 41]. The method of obtaining an elastic implant by electrospinning contributes to the creation of a voluminous fibrous framework with a fiber diameter and interfiber gaps that are optimal for cell and vessel migration [42]. It was revealed that post-traumatic changes in the joints and the development of osteoarthritis are associated with the temperature of the skin in the joint area. At the same time, the severity of the pain syndrome does not correlate with pain sensations of the patient [43].

In our study, skin temperature in the area of the knee joint was increased in the early postoperative period and persisted up to 2 weeks of the experiment, what was associated with the post-traumatic state of tissues after surgery [44]. In the control series, a significantly increased temperature was noted after one year of observation and was associated with an aggravation of the arthritic changes, what was confirmed by anatomical and histological methods [44-46]. A slight increase in the skin temperature in the animals

of the experimental series, compared with the control one, we associate with the improvement of microcirculation in the restored tissues in the area of damage. It was observed in the works of other researchers [47, 48].

Throughout the experiment, the volume of limb soft tissues in the animals of the experimental series was higher than in the animals of the control series. MRI used by several studies revealed a decrease in limb circumference in patients with gonarthrosis, associated with reduction in the muscle diameter and replacement of muscle tissue with adipose tissue [49].

The range of joint motion in the series with replacement of an osteochondral defect with a PLC matrix impregnated with hydroxyapatite at all stages of the experiment, especially in long-term periods (six months and a year of observation) was significantly better than in the animals of the control series. We attribute this to the progression of osteoarthritis signs in the control series. The reduced range of motion in the knee joint can be explained by pain and discomfort by walking and joint loading [50-52]. Restoration of the anatomical integrity and complete organotypicity of the newly formed regenerate in the area of the osteochondral defect in the experimental series already after 180 days of observation, proven by anatomical and histological methods, in our opinion, is associated with the structure of the implant, its good adhesive ability, sufficient porosity and elasticity. Starting from the moment of surgery, the elastic implant filled the area of the osteochondral defect, ensuring the integrity and congruence of the articular surface, withstanding the functional load, that is providing factors that are considered important in the healing of osteochondral defects [53, 54].

Early functional loading contributed to the ingrowth of microvessels into micropores between the fibers of the implant. Perivascular cells and bone marrow cells attached to the structured surface of the implant, thanks to the hydroxyapatite nanoparticles deposited on them. Hydroxyapatite acted as an inducer of osteogenesis and promoted cell differentiation along the osteogenic pathway [55]. Since the vessels grew into the implant from the side of the intact subchondral bone, the formation of bone tissue occurred in the projection of the cancellous bone surrounding the defect, which is necessary as a base and nourishing factor for the formation of cartilage tissue on the surface. There were no vessels in the surface layers of the implant. Under such conditions, undifferentiated bone marrow cells penetrating the surface in the projection of the articular cartilage surrounding the defect differentiated along the chondrogenic pathway. Cell differentiation into chondroblasts and chondrocytes continued throughout the experiment with sufficient nutrition from the synovium, which produced a sufficient volume

of synovial fluid, because animals actively used the limb.

These mechanisms contributed to the complete replacement of the biodegradable implant with tissues of a typical structure by experiment day 180. By that period, cancellous bone with a cartilaginous hyalin-like lining was formed on the surface of the defect in the projection of the subchondral bone.

It was found that with an increase in the osteoarthritis severity according to the classification of the International Cartilage Restoration Society (ICRS), cartilage stiffness decreases, which is primarily affected by the integrity of the extracellular matrix. Therefore, methods to study stiffness, such as impression, can be used to characterize cartilage in all stages of OA [56].

The study of stiffness in patients after the treatment of osteochondral defects by implantation of autologous chondrocytes (ACI) into the area of damage to the cartilage surface showed the restoration of the stiffness of the newly

formed tissue regenerate 2 years after implantation and a further increase in this indicator within 5 years [57]. In our study, the restoration of biomechanical compliance (analogous to stiffness) in the experimental group reached the parameters of intact animals after 60 days of the experiment and persisted throughout the year of observation. It remained lower by 27-29 % during the entire observation period in the control group.

In this experiment, we applied a strategy based on the fact that an elastic PCL implant with hydroxyapatite imitated the extracellular matrix, which promoted the growth, proliferation, and differentiation of cells in the area of the osteochondral defect, using the self-regenerative potential of cells and its interaction with biomolecules [58]. Our study showed that the mechanical properties of the cartilage in the experimental group restored to the level of the intact animals by day 60 and persisted up to 360 days, while in the control group they did not restore even after 360 days.

## CONCLUSION

A biodegradable elastic implant produced with the method of electrospinning from polycaprolactone and impregnated with hydroxyapatite could potentially be used to treat osteochondral defects. This type of implant

provided repair of the tissues in the osteochondral defect area and regeneration of both the articular cartilage and subchondral bone.

**Funding** This research received no external funding

**Institutional Review Board Statement** The study was conducted in accordance with the Declaration of Helsinki, and approved by the Ethics Committee of the Ilizarov National Medical Research Center for Traumatology and Orthopedics, Kurgan, Russia (protocol code 1(71), date of approval 28 April 2022).

**Data Availability Statement** Data are available upon a demand to corresponding author (D.P.).

**Conflicts of Interest** The authors declare no conflicts of interest.

## REFERENCES

- Airapetov GA, Vorotnikov AA, Konovalov EA. Surgical methods of focal hyaline cartilage defect management in large joints (literature review). *Genij Ortopedii*. 2017;23(4):485-491. doi: 10.18019/1028-4427-2017-23-4-485-49
- Pearsall IV A, Madanagopal S, Tucker J. The Evaluation of Refrigerated and Frozen Osteochondral Allografts in the Knee. *Surgical Science*. Vol. 2011;2(5):232-241. doi: 10.4236/ss.2011.25052
- Bryanskaya AI, Tikhilov RM, Kulyaba TA, Kornilov NN. Surgical treatment of patients with local defects of joint surface of femur condyles (review). *Traumatology and Orthopedics of Russia*. 2010;16(4):84-92. (In Russ.) doi: 10.21823/2311-2905-2010-0-4-84-92
- Sovetnikov NN, Kalsin VA, Konoplyannikov MA, Mukhanov VV. Cell technologies and tissue engineering in the treatment of articular chondral defects. *Clinical practice*. 2013;1(1):52-66. (In Russ.)
- Bozhokin M.S., Bozhkova S.A., Netylko G.I. Possibilities of current cellular technologies for articular cartilage repair (analytical review). *Traumatology and Orthopedics of Russia*. 2016;22(3):122-134. (In Russ.) doi: 10.21823/2311-2905-2016-22-3-122-134
- Hafezi-Nejad N, Zikria B, Eng J, et al. Predictive value of semi-quantitative MRI-based scoring systems for future knee replacement: data from the osteoarthritis initiative. *Skeletal Radiol*. 2015;44(11):1655-1662. doi: 10.1007/s00256-015-2217-2
- Kulyaba TA, Bantser SA, Trachuk PA, et al. The Effectiveness of Various Surgical Techniques in the Treatment of Local Knee Cartilage Lesions (Review). *Traumatology and Orthopedics of Russia*. 2020;26(3):170-181. doi: 10.21823/2311-2905-2020-26-3-170-181
- Richter DL, Schenck RC Jr, Wascher DC, Treme G. Knee Articular Cartilage Repair and Restoration Techniques: A Review of the Literature. *Sports Health*. 2016;8(2):153-160. doi: 10.1177/1941738115611350
- Kotelnikov G.P., Volova L.T., Lartsev y.V., Dolgushkin D.A., Terteryan M.A. The new plastic method of articular hyaline cartilage defects with combined cellular-tissue graft. *Traumatology and Orthopedics of Russia*. 2010;1(1):150-155. (In Russ.) doi: 10.21823/2311-2905-2010-0-1-150-155
- Matsusue Y, Kotake T, Nakagawa Y, Nakamura T. Arthroscopic osteochondral autograft transplantation for chondral lesion of the tibial plateau of the knee. *Arthroscopy*. 2001;17(6):653-659. doi: 10.1053/jars.2001.22400
- Kulyaba TA, Kornilov NN, Selin AV, Pechinskij AI. Long-term results of mosaic osteochondral autoplasty in the treatment of diseases and injuries of the knee joint. *Traumatology and Orthopedics of Russia*. 2007;3(3):24. (In Russ.)
- Filardo G, Kon E, Roffi A, et al. Scaffold-based repair for cartilage healing: a systematic review and technical note. *Arthroscopy*. 2013;29(1):174-186. doi: 10.1016/j.arthro.2012.05.891
- Schrock JB, Kraeutler MJ, Houck DA, et al. A Cost-Effectiveness Analysis of Surgical Treatment Modalities for Chondral Lesions of the Knee: Microfracture, Osteochondral Autograft Transplantation, and Autologous Chondrocyte Implantation. *Orthop J Sports Med*. 2017;5(5):2325967117704634. doi: 10.1177/2325967117704634
- Christensen BB, Foldager CB, Jensen J, et al. Poor osteochondral repair by a biomimetic collagen scaffold: 1- to 3-year clinical and radiological follow-up. *Knee Surg Sports Traumatol Arthrosc*. 2016;24(7):2380-7. doi: 10.1007/s00167-015-3538-3
- Nair LS, Laurencin CT. Biodegradable polymers as biomaterials. *Prog Polym Sci*. 2007;32(8-9):762-798. doi: 10.1016/j.progpolymsci.2007.05.017



16. Kozadaev MN. The use of polycaprolactone-based matrices to stimulate the regeneration of articular cartilage under experimental conditions. *Theoretical and applied aspects of modern science*. 2014;(3-2):128-130. (In Russ.)
17. Filardo G, Kon E, Roffi A, et al. Scaffold-based repair for cartilage healing: a systematic review and technical note. *Arthroscopy*. 2013;29(1):174-86. doi: 10.1016/j.arthro.2012.05.891
18. Mohan N, Nair PD. A synthetic scaffold favoring chondrogenic phenotype over a natural scaffold. *Tissue Eng Part A*. 2010;16(2):373-84. doi: 10.1089/ten.TEA.2009.0314
19. Levingstone TJ, Ramesh A, Brady RT, et al. Cell-free multi-layered collagen-based scaffolds demonstrate layer specific regeneration of functional osteochondral tissue in caprine joints. *Biomaterials*. 2016;87:69-81. doi: 10.1016/j.biomaterials.2016.02.006
20. Nirmal RS, Nair PD. Significance of soluble growth factors in the chondrogenic response of human umbilical cord matrix stem cells in a porous three dimensional scaffold. *Eur Cell Mater*. 2013;26:234-251. doi: 10.22203/ecm.v026a17
21. Hernigou J, Vertongen P, Chahidi E, et al. Effects of press-fit biphasic (collagen and HA/ $\beta$ TCP) scaffold with cell-based therapy on cartilage and subchondral bone repair knee defect in rabbits. *Int Orthop*. 2018;42(7):1755-1767. doi: 10.1007/s00264-018-3999-3
22. Meng X, Ziadlou R, Grad S, et al. Animal Models of Osteochondral Defect for Testing Biomaterials. *Biochem Res Int*. 2020;2020:9659412. doi: 10.1155/2020/9659412
23. van den Borne MP, Raijmakers NJ, Vanlauwe J, et al. International Cartilage Repair Society (ICRS) and Oswestry macroscopic cartilage evaluation scores validated for use in Autologous Chondrocyte Implantation (ACI) and microfracture. *Osteoarthritis Cartilage*. 2007;15(12):1397-1402. doi: 10.1016/j.joca.2007.05.005
24. Guo X, Park H, Young S, et al. Repair of osteochondral defects with biodegradable hydrogel composites encapsulating marrow mesenchymal stem cells in a rabbit model. *Acta Biomater*. 2010;6(1):39-47. doi: 10.1016/j.actbio.2009.07.041
25. Caminal M, Moll X, Codina D, et al. Transitory improvement of articular cartilage characteristics after implantation of polylactide:polyglycolic acid (PLGA) scaffolds seeded with autologous mesenchymal stromal cells in a sheep model of critical-sized chondral defect. *Biotechnol Lett*. 2014;36(10):2143-2153. doi: 10.1007/s10529-014-1585-3
26. Zheng P, Hu X, Lou Y, Tang K. A Rabbit Model of Osteochondral Regeneration Using Three-Dimensional Printed Polycaprolactone-Hydroxyapatite Scaffolds Coated with Umbilical Cord Blood Mesenchymal Stem Cells and Chondrocytes. *Med Sci Monit*. 2019;25:7361-7369. doi: 10.12659/MSM.915441
27. O'Driscoll SW, Keeley FW, Salter RB. The chondrogenic potential of free autogenous periosteal grafts for biological resurfacing of major full-thickness defects in joint surfaces under the influence of continuous passive motion. An experimental investigation in the rabbit. *J Bone Joint Surg Am*. 1986;68(7):1017-1035.
28. Moojen DJ, Saris DB, Auw Yang KG, et al. The correlation and reproducibility of histological scoring systems in cartilage repair. *Tissue Eng*. 2002;8(4):627-634. doi: 10.1089/107632702760240544
29. Rutgers M, van Pelt MJ, Dhert WJ, et al. Evaluation of histological scoring systems for tissue-engineered, repaired and osteoarthritic cartilage. *Osteoarthritis Cartilage*. 2010;18(1):12-23. doi: 10.1016/j.joca.2009.08.009
30. McGoldrick NP, Murphy EP, Kearns SR. Osteochondral lesions of the ankle: The current evidence supporting scaffold-based techniques and biological adjuncts. *Foot Ankle Surg*. 2018;24(2):86-91. doi: 10.1016/j.fas.2017.01.003
31. Dorotka R, Windberger U, Macfelda K, et al. Repair of articular cartilage defects treated by microfracture and a three-dimensional collagen matrix. *Biomaterials*. 2005;26(17):3617-3629. doi: 10.1016/j.biomaterials.2004.09.034
32. Schüttler KF, Schenker H, Theisen C, et al. Use of cell-free collagen type I matrix implants for the treatment of small cartilage defects in the knee: clinical and magnetic resonance imaging evaluation. *Knee Surg Sports Traumatol Arthrosc*. 2014;22(6):1270-1276. doi: 10.1007/s00167-013-2747-x
33. Roessler PP, Pfister B, Gesslein M, et al. Short-term follow up after implantation of a cell-free collagen type I matrix for the treatment of large cartilage defects of the knee. *Int Orthop*. 2015;39(12):2473-2479. doi: 10.1007/s00264-015-2695-9
34. Irawan V, Sung TC, Higuchi A, Ikoma T. Collagen Scaffolds in Cartilage Tissue Engineering and Relevant Approaches for Future Development. *Tissue Eng Regen Med*. 2018;15(6):673-697. doi: 10.1007/s13770-018-0135-9
35. De Santis R, Russo A, Gloria A, et al. Towards the Design of 3D Fiber-Deposited Poly( $\epsilon$ -caprolactone)/Iron-Doped Hydroxyapatite Nanocomposite Magnetic Scaffolds for Bone Regeneration. *J Biomed Nanotechnol*. 2015;11(7):1236-46. doi: 10.1166/jbn.2015.2065
36. Domingos M, Intraruovo F, Russo T, et al. The first systematic analysis of 3D rapid prototyped poly( $\epsilon$ -caprolactone) scaffolds manufactured through BioCell printing: the effect of pore size and geometry on compressive mechanical behaviour and in vitro hMSC viability. *Biofabrication*. 2013;5(4):045004. doi: 10.1088/1758-5082/5/4/045004
37. Chen J, Chen H, Li P, et al. Simultaneous regeneration of articular cartilage and subchondral bone in vivo using MSCs induced by a spatially controlled gene delivery system in bilayered integrated scaffolds. *Biomaterials*. 2011;32(21):4793-4805. doi: 10.1016/j.biomaterials.2011.03.041
38. Chen Y, Liu X, Liu R, et al. Zero-order controlled release of BMP2-derived peptide P24 from the chitosan scaffold by chemical grafting modification technique for promotion of osteogenesis in vitro and enhancement of bone repair in vivo. *Theranostics*. 2017;7(5):1072-1087. doi: 10.7150/thno.18193
39. Wu X, Miao L, Yao Y, et al. Electrospun fibrous scaffolds combined with nanoscale hydroxyapatite induce osteogenic differentiation of human periodontal ligament cells. *Int J Nanomedicine*. 2014;9:4135-43. doi: 10.2147/IJN.S65272
40. Ronca D, Langella F, Chierchia M, et al. Bone Tissue Engineering: 3D PCL-based Nanocomposite Scaffolds with Tailored Properties. *Procedia CIRP*. 2016;49:51-54. doi: 10.1016/j.procir.2015.07.028
41. Domingos M, Gloria A, Coelho J, et al. Three-dimensional printed bone scaffolds: The role of nano/micro-hydroxyapatite particles on the adhesion and differentiation of human mesenchymal stem cells. *Proc Inst Mech Eng H*. 2017;231(6):555-564. doi: 10.1177/0954411916680236
42. Ginestra P, Ceretti E, Fiorentino A. Electrospinning of Poly-caprolactone for Scaffold Manufacturing: Experimental Investigation on the Process Parameters Influence. *Procedia CIRP*. 2016;49:8-13. doi: 10.1016/j.procir.2015.07.020
43. Alfieri FM, Vargas E Silva NCO, Dos Santos ACA, Battistella LR. Cutaneous temperature and pressure pain threshold in individuals with knee osteoarthritis. *Reumatologia*. 2020;58(5):272-276. doi: 10.5114/reum.2020.100195
44. Windisch C, Brodt S, Röhner E, Matziolis G. Effects of Kinesio taping compared to arterio-venous Impulse System™ on limb swelling and skin temperature after total knee arthroplasty. *Int Orthop*. 2017;41(2):301-307. doi: 10.1007/s00264-016-3295-z
45. Edrich J, Smyth CJ. Arthritis inflammation monitored by subcutaneous millimeter wave thermography. *J Rheumatol*. 1978 Spring;5(1):59-67.
46. Oblinger W, Engel JM, Franke M. Thermographische Diagnostik der Arthritis peripherer Gelenke [Thermographic diagnosis of arthritis in peripheral joints]. *Z Rheumatol*. 1985;44(2):77-81. (In German)
47. Windisch C, Brodt S, Roehner E, Matziolis G. Regional differences in temperature course after knee arthroplasty. *Knee Surg Sports Traumatol Arthrosc*. 2016;24(8):2686-2691. doi: 10.1007/s00167-015-3809-z
48. Windisch C, Brodt S, Röhner E, Matziolis G. Effects of Kinesio taping compared to arterio-venous Impulse System™ on limb swelling and skin temperature after total knee arthroplasty. *Int Orthop*. 2017;41(2):301-307. doi: 10.1007/s00264-016-3295-z
49. Mohajer B, Dolatshahi M, Moradi K, et al. Role of Thigh Muscle Changes in Knee Osteoarthritis Outcomes: Osteoarthritis Initiative Data. *Radiology*. 2022;305(1):169-178. doi: 10.1148/radiol.212771
50. Egloff C, Hügler V, Valderrabano V. Biomechanics and pathomechanisms of osteoarthritis. *Swiss Med Wkly*. 2012;142:w13583. doi: 10.4414/smw.2012.13583
51. Wojcieszek A, Kurowska A, Majda A, et al. The Impact of Chronic Pain, Stiffness and Difficulties in Performing Daily Activities on the Quality of Life of Older Patients with Knee Osteoarthritis. *Int J Environ Res Public Health*. 2022;19(24):16815. doi: 10.3390/ijerph192416815
52. Kiss RM. Effect of severity of knee osteoarthritis on the variability of gait parameters. *J Electromyogr Kinesiol*. 2011;21(5):695-703. doi: 10.1016/j.jelekin.2011.07.011

53. Popkov AV, Popkov DA, Kobzyev AE, et al. Positive experience of full-layer filling of articular cartilage defect using a degradable implant with a bioactive surface in combination with platelet-rich blood plasma (experimental study). *Genij Ortopedii*. 2020;26(3):392-397. doi: 10.18019/1028-4427-2020-26-3-392-397
54. Dahlin RL, Kinard LA, Lam J, et al. Articular chondrocytes and mesenchymal stem cells seeded on biodegradable scaffolds for the repair of cartilage in a rat osteochondral defect model. *Biomaterials*. 2014;35(26):7460-7469. doi: 10.1016/j.biomaterials.2014.05.055
55. Christensen BB, Foldager CB, Hansen OM, et al. A novel nano-structured porous polycaprolactone scaffold improves hyaline cartilage repair in a rabbit model compared to a collagen type I/III scaffold: in vitro and in vivo studies. *Knee Surg Sports Traumatol Arthrosc*. 2012;20(6):1192-1204. doi: 10.1007/s00167-011-1692-9
56. Kleemann RU, Krockner D, Cedraro A, et al. Altered cartilage mechanics and histology in knee osteoarthritis: relation to clinical assessment (ICRS Grade). *Osteoarthritis Cartilage*. 2005;13(11):958-963. doi: 10.1016/j.joca.2005.06.008
57. Paatela T, Vasara A, Nurmi H, et al. Biomechanical Changes of Repair Tissue after Autologous Chondrocyte Implantation at Long-Term Follow-Up. *Cartilage*. 2021;13(1\_suppl):1085S-1091S. doi: 10.1177/1947603520921433
58. Maia FR, Carvalho MR, Oliveira JM, Reis RL. Tissue Engineering Strategies for Osteochondral Repair. *Adv Exp Med Biol*. 2018;1059:353-371. doi: 10.1007/978-3-319-76735-2\_16

The article was submitted 15.09.2023; approved after reviewing 25.09.2023; accepted for publication 01.10.2023.

**Information about the authors:**

- 1 Arnold V. Popkov – Doctor of Medical Sciences, Professor, Chief Researcher, apopkov.46@mail.ru, <https://orcid.org/0000-0001-5791-1989>;
- 2 Evgenii S. Gorbach – traumatologist-orthopedist, gorbach.evg@mail.ru, <https://orcid.org/0000-0002-0682-1825>;
- 3 Elena Gorbach N. – Candidate of Biological Sciences, Leading Researcher, gorbach.e@mail.ru, <https://orcid.org/0000-0002-9516-7481>;
- 4 Natalia A. Kononovich – Candidate of Veterinary Sciences, Leading Researcher, n.a.kononovich@mail.ru, <https://orcid.org/0000-0002-5990-8908>;
- 5 Elena A. Kireeva – Candidate of Biological Sciences, Junior Researcher, ea\_tkachuk@mail.ru, <https://orcid.org/0000-0002-1006-5217>;
- 6 Dmitry A. Popkov – Doctor of Medical Sciences, Professor of the Russian Academy of Sciences, Corresponding Member of the French Academy of Medical Sciences, Head of the Clinic, dpopkov@mail.ru, <https://orcid.org/0000-0002-8996-867X>.

**Contribution of the authors:**

Popkov AV – Conceptualization, supervision, project administration.  
Gorbach ES – Conceptualization, formal analysis, investigation, visualization.  
Gorbach EN – investigation.  
Kononovich NA – validation, writing–original draft preparation.  
Kireeva EA – data curation.  
Popkov DA – formal analysis, writing–review and editing.  
All authors have read and agreed to the published version of the manuscript.